Available online at www.sciencedirect.com

ScienceDirect

journal homepage: www.elsevier.com/locate/he

[redacted]

Chi Yu [a,b], Shuanshi Fan [a,b,*], Xuemei Lang [a,b], Yanhong Wang [a,b], Gang Li [a,b], Shenglong Wang [a,b]

a [redacted]

b [redacted]

HIGHLIGHTS

- Achieving high capacity hydrogen energy storage in gas hydrate at mild conditions.
- Chemical energy in the additives dramatically increase total energy storage density.
- Mechanism of tBA promote hydrate-based H_2 storage was studied by Raman spectroscopy.

GRAPHICAL ABSTRACT

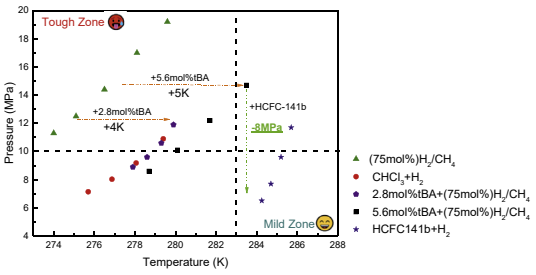

ARTICLE INFO

[redacted]:
Received 11 February 2020
Received in revised form
26 March 2020
Accepted 28 March 2020
Available online 18 April 2020

[redacted]:
Hydrogen storage
Gas hydrate
Hybrid energy storage
Hydrate phase equilibrium
Raman spectroscopy

ABSTRACT

Hydrogen storage in clathrate hydrates is a promising approach for industry-scale utilizations. However, extreme operation conditions such as high pressure (about GPa) limit the development. In this work hydrogen hydrate phase equilibrium in addition of methane, tert-butyl alcohol (tBA), trichloromethane ($CHCl_3$) and 1,1-dichloro-1-fluoroethane (HCFC-[redacted]286 K, which including 21 points in total. Meanwhile, spectroscopic studies using Raman spectroscopy show that tBA and H[redacted]$_2$O form metastable hydrate cages via hydrogen bonds, then form stable sII hydrates with the help of CH_4. Hydrate-based hydrogen storage capacity in 5.6 mol%HCFC-141 b-water mixture could reach 46 V/V (0.36 wt%) at 273 K and 10 MPa. Combing with chemical energy of HCFC-141 b, this work achieved high capacity of hydrogen and chemical energy storage in gas hydrate at mild conditions. This study will provide guidance on hydrate-chemical hybrid hydrogen storage technology, and leads to the next generation of hybrid hydrate-based hydrogen technology in the future.

* [redacted]. School of Chemistry and Chemical Engineering, South China University of Technology, Guangzhou, China.
E-mail address: ssfan@scut.edu.cn (S. Fan).

https://doi.org/10.1016/j.ijhydene.2020.03.228

Gas hydrates is clathrate compound formed by water (host molecule) and gas (guest molecule) under high pressure and low temperature. Gas hydrates reservoir is a promising energy resource, exploration and gas production of it has been studied [1,2]. Meanwhile gas hydrate is a good energy material, hydrated-based technology has been applied on gas storage [3] and hydrogen purification from syngas [4,5]. Hydrogen storage in clathrate hydrates is a promising hydrogen storage technology with large scale industrial application prospects [6–9]. For further improving hydrogen storage properties, there are three generations of hydrate-based hydrogen storage technology have been developed. The first generations was using hydrogen hydrate (structure II) as hydrogen storage material. Mao et al. [10,11]reported hydrogen storage capacity could reach 5.26 wt% when hydrogen formation at 180–220 MPa and 300 K, which is higher than 2020 DOE's target (4.5 wt%).

The second generation was using energy-free liquid or solid additives in hydrate-based hydrogen storage, aiming to lower hydrate phase equilibrium conditions. Weissman et al. [12] studied 5.56 mol% tetrahydrofuran (THF)+ hydrogen + water hydrate forming at 274 K, 6.89 MPa and 274 K, 11 MPa, hydrogen storage capacity was lower than 1 wt % and hydrogen only occupied 5^{12} cage of the gas hydrate. Liu et al. [13] using Ab initio molecular dynamic simulation studied cage occupation of H_2 and THF in H_2+THF hydrate at 140 K, and theoretical hydrogen storage could reach 1.6 wt% and 3.8 wt% by calculation. Di Profio et al. [14] using THF reverse micelles to enhance the kinetics of the formation process and assist clathrate formation, hydrogen capacity could reach 0.5 wt% within 28min. Kaur et al. [15] examines the host-guest interactions in H_2-THF mix hydrate by computational study which proves H_2 molecules can be occupied in the hexakaidecahedral cages along with THF as well as single occupied in small cages. Trueba et al.[[16,17]] studied tetrabutylammonium bromide (TBAB) and tetrabutylammonium fluoride (TBAF) thermodynamically promote hydrate-based hydrogen storage, hydrogen capacity are lower than 0.1 wt%.

The third generation was using flammable gas molecules as promoters in hydrate-based hydrogen storage, aiming to increase totally energy storage density. Veluswamy et al. [18,19] studied propane promoting hydrate-based hydrogen storage and tested hydrate phase equilibrium of hydrogen-propane binary hydrate. Matsumoto et al. [20] using in-situ Raman spectra studied methane promoting hydrate-based hydrogen storage, maximum hydrogen storage capacity achieved 0.31 wt% at 263 K and 70 MPa. Zhang et al. [21] studied growth of H_2 + CH_4 binary hydrates via molecular dynamic simulation, results shown that the solubility and diffusivity of guest molecules especially CH_4 dominate the growth process.

However, hydrogen storage capacity of the second and third generations hydrate-based hydrogen storage technology still quite low in ambient temperature and low pressure (lower than 25 MPa). Aiming to lower hydrate formation condition and increase hydrogen energy storage capacity simultaneously, this paper proposes a novel approach that using materials containing chemical hydrogen energy as hydrate formation promoters. In this work hydrogen hydrate phase equilibrium in addition of methane + tert-butyl alcohol (tBA), trichloromethane ($CHCl_3$) and 1,1-dichloro-1-fluoroethane (HCFC-141 b) were tested, and enclathration mechanism of hydrogen + methane + tBA were studied via Raman spectroscopy. This study will provide guidance on hydrate-chemical hybrid hydrogen storage technology, and leads to the next generation of hybrid hydrate-based hydrogen technology in the future.

Experimental apparatus of hydrate phase equilibrium were detailed described in previous work [22–25]. The key parts of this apparatus is a 300 mL stirred high pressure vessel with a cold bath to control temperature. Two thermocouples monitored temperature of gas and liquid phase inside the vessel. A pressure sensor measured pressure of the apparatus. All data were recorded by Agilent 34970 A data logger. Experimental method of hydrate phase equilibrium is like previous work [22,23]. Tert-butyl alcohol (tBA, > 98%, Jiangsu Yonghua Chemical Technology Co.) was diluted as 2.8 mol% tBA (aq) and 5.6 mol% tBA (aq), trichloromethane ($CHCl_3$, > 98% Guangzhou Chemical Reagent Co.) and 1,1-dichloro-1-fluoroethane (HCFC-141 b, > 98% Pujiang Jietong Environmental Protection Technology Co.) were mixture with DI water to 5.6 mol% $CHCl_3$-water mixture and 5.6 mol% HCFC-141 b-water mixture respectively. 200 mL experimental solution (or mixture) was inhaled into the vessel, and then tested gas was pumped into vessel to the desired pressure. After that started stirrer (about 600 rpm) and temperature control. The temperature control program was as following: Firstly, cooling down with a rate of 3 K/h to hydration formation region and constant temperature about 3 h for hydrate formation, then heat up with 0.1 K/h. Monitored pressure change of hydrate dissociation line, change the heating rate to 0.025 K/h when the pressure drop of hydrate formation line and hydrate dissociation line in P-T curve was smaller than 0.5 MPa. The intersection point of the hydrate formation line and hydrate dissociation line in P-T curve was considered to the hydrate phase equilibrium points.

Hydrate-based hydrogen storage of experiments of H_2 storage in 5.6 mol% HCFC-141 b-water mixture used same apparatus but with stirred speed of 300 rpm. Experiment process was described as follows: Firstly, washing the vessel with DI water. After that cooling the vessel to 270 K–273 K, injected 100 mL 5.6 mol% HCFC-141 b-water mixture. Turn on the stirring (300 rpm) and keep the reaction vessel constant to 273 K, then injected H_2 into the reactor to the target pressure and started data collection. While — < 0.01 /(•) considered that the reaction was complete and reached total hydrogen storage capacity.

Raman spectrum was conducted at ThermoFisher DXR2xi Raman spectroscopy. Laser wavelength was 532 nm, laser power was 9.5 mW, exposure time was 0.02s. To precisely control test temperature, a FTIR6000 cold stage manufactured by LINKEN was used during the test. Test temperature of Raman spectra was −100 °C.

(1) Enclathration of tert-butyl alcohol in (75 mol%)H_2/CH_4 hydrate

5.6 mol% tBA (aq) represents all $5^{12}6^4$ cages were occupied by tBA molecule while forming sII gas hydrate, and 2.8 mol% tBA (aq) represents half of $5^{12}6^4$ cages were occupied by tBA molecule while forming sII gas hydrate. Hydrate phase equilibrium data of (75 mol%)H_2/CH_4+water and (75 mol%)H_2/CH_4+tBA (aq) are demonstrated in Table 1 and Fig. 1.

Fig. 1 and Table 1 shown that comparing to hydrate phase equilibrium line of (75 mol%)H_2/CH_4 +water, 5.6 mol% tBA and 2.8 mol% tBA shifted the hydrate phase equilibrium line of (75 mol%)H_2/CH_4 about 4 K and 5 K towards higher temperature, respectively. Increasing concentration of tBA from 0 mol % to 2.8 mol%, hydrate formation is significantly thermodynamically enhanced (Fig. 1). While tBA concentration continually increasing from 2.8 mol% to 5.6 mol%, hydrate phase equilibrium line shifted 1 K towards higher temperature. This phenomenon indicated that existence of tBA molecule could help gas molecules and water to clathrate gas hydrate.

In order to explore the mechanism of tBA thermodynamics promoting the formation of hydrogen hydrate, Raman spectra of tBA and tBA solutions at −100 °C were conducted and results shown in Fig. 2. Firstly, the characteristic peaks of C–C bonds stretching vibration with Raman shifts of 500 cm^{-1}-1500 cm^{-1} are consistent for both tBA and tBA solutions at −100 °C, which indicates that the molecular structure of tBA has not changed in tBA solution. Secondly, the C–H stretching vibration peak of Raman shift 2800 cm^{-1}-2950 cm^{-1} is highly coincident with the C–H vibration peak of alkane molecules such as methane in hydrate cages [26]. It was found that for the tBA of −100 °C, C–H vibration peaks of 5.6 mol%tBA (aq) and 2.8 mol%tBA (aq) in the range of 2800 cm $^{-1}$-2950 cm^{-1} were slightly shifted to low Raman shift direction by about 30 cm^{-1}. This phenomenon is highly consistent with the C–H bond Raman shift phenomenon when alkanes such as methane form gas hydrates. Finally, the change in the –OH vibration peak in the region indicated by the green dashed line in Fig. 2 shows that the water molecules form a cage structure (hydrate or ice) at low temperature in the tBA solution. Based on the above three characteristics of Raman spectra, it is concluded that tBA affect H-bond of water molecule, induce water molecule to form clathrate cages which leads to the change of –OH characteristic peaks. At the same time the movement of tBA molecules from bulk solution into the hydrate cages participates in the formation of hydrates, resulting in the change of C–H bonds vibration peaks.

Combining the conclusion of the differences between Raman spectra of tBA and tBA solutions (Fig. 2) and the results of Kim et al. [27], the mechanism of tBA molecule thermodynamically promote formation of (75 mol%)H_2/CH_4 hydrate is shown in Fig. 3: Firstly tBA acts as guest molecule induces water molecules forming metastable $5^{12}6^4$ cages (Fig. 3a) through H-bond between water and hydroxyl groups of tBA. And then with the help of methane molecule, stable sII hydrate are formed (Fig. 3b). Lastly hydrogen molecules move into hydrate phase (Fig. 3c). It is the core process that tBA forms metastable $5^{12}6^4$ cages thermodynamically promoted (75 mol%)H_2/CH_4 hydrate formation.

(2) Thermodynamically promotion of 1,1-dichloro-1-fluoroethane and trichloromethane

In order to further reduce the pressure of hydrate-based hybrid hydrogen storage, the thermodynamically promotion effect of 1,1-dichloro-1-fluoroethane (HCFC-141 b) and chloroform ($CHCl_3$) on hydrate based hydrogen storage was studied. Halogen group (-Cl or –F) in halo hydrocarbons enhances the van der Waals force between guest molecules and water. Hydrate phase equilibrium data of $CHCl_3$+H_2+water and HCFC141b + H_2+water are demonstrated in Table 2 , Table 3 and Fig. 4.

Table 2 and Fig. 4 shown hydrate phase equilibrium of $CHCl_3$+H_2 hydrate in the range of 275 K–280 K, 7 MPã11 MPa, which is significant lower than hydrogen hydrate [28]. Fig. 4 shown that compared with (75 mol%)H_2/CH_4 hydrate phase equilibrium line, $CHCl_3$+H_2 hydrate phase equilibrium line shifts about 5 K toward higher temperature. The molecular size of $CHCl_3$ is similar to methane, the difference is three Cl atoms replaced three H atoms in CH_4 molecules. Three -Cl groups in $CHCl_3$ influence the hydrogen bond among water molecules and affects the H-bond of H–O–H which induce and change the order of hydrogen bonding between water molecules. The van der Waals force between $CHCl_3$ molecules and water molecules are reinforced. As consequences of that, it is thermodynamically easier for $CHCl_3$ to form a hydrate cage with water and promote the formation of hydrogen hydrate.

Table 3 and Fig. 4 shown that hydrate phase equilibrium of HCFC141b + H_2 hydrate which in the range of 284 K–286 K, 5 MPã12 MPa, is significant lower than hydrogen hydrate [28]. Fig. 4 shown that compared with (75 mol%)H_2/CH_4 hydrate phase equilibrium line, HCFC141b + H_2 hydrate phase equilibrium line shifts about 10 K toward higher temperature. In contrast, the hydrate phase equilibrium line of HCFC-141 b + H_2 hydrate is more sensitive to temperature change. A small increase in temperature can cause a significant increase in phase equilibrium pressure. The above results indicate that

1 – , (75 %) 2/ 4+5.6 % ( ) (75 %) 2/ 4+2. % ( ).

System components	Temperature (K)	Pressure (MPa)
(75 mol%)H_2/CH_4+water	274.0 ± 0.1 K	11.3 ± 0.1 MPa
	275.1 ± 0.1 K	12.5 ± 0.1 MPa
	276.5 ± 0.1 K	14.4 ± 0.1 MPa
	278.1 ± 0.1 K	17.0 ± 0.1 MPa
	279.6 ± 0.1 K	19.2 ± 0.1 MPa
(75 mol%)H_2/CH_4+5.6 mol% tBA (aq)	278.7 ± 0.1 K	8.6 ± 0.1 MPa
	280.1 ± 0.1 K	10.1 ± 0.1 MPa
	281.7 ± 0.1 K	12.2 ± 0.1 MPa
	283.5 ± 0.1 K	14.7 ± 0.1 MPa
(75 mol%)H_2/CH_4+2.8 mol% tBA (aq)	277.9 ± 0.1 K	8.9 ± 0.1 MPa
	278.6 ± 0.1 K	9.6 ± 0.1 MPa
	279.3 ± 0.1 K	10.6 ± 0.1 MPa
	279.9 ± 0.1 K	11.9 ± 0.1 MPa

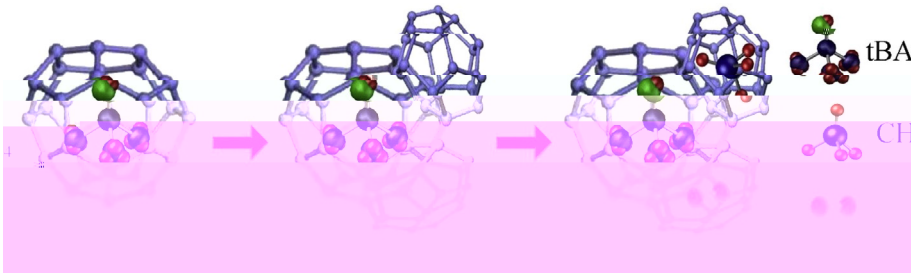

. 3 – (75 %) 2/ 4 .

2 –
3+ 2+ .

Temperature (K)	Pressure (MPa)
279.4 ± 0.1 K	10.9 ± 0.1 MPa
278.1 ± 0.1 K	9.2 ± 0.1 MPa
276.9 ± 0.1 K	8.0 ± 0.1 MPa
275.7 ± 0.1 K	7.1 ± 0.1 MPa

3 –
141 + 2+ .

Temperature (K)	Pressure (MPa)
284.3 ± 0.1 K	6.5 ± 0.1 MPa
284.7 ± 0.1 K	7.7 ± 0.1 MPa
285.2 ± 0.1 K	9.6 ± 0.1 MPa
285.7 ± 0.1 K	11.7 ± 0.1 MPa

The commonality of HCFC-141 b and $CHCl_3$ is both have three halogenated groups linked to one carbon atom. The differences are follows: (1) There are one –F group and 2 -Cl groups in HCFC-141 b while there are three -Cl groups in $CHCl_3$, and (2) there is one more carbon in HCFC-141 b than that in $CHCl_3$. Concluding from the results it is considered that guest molecular with –F group is better than with -Cl on thermodynamically promoting hydrate-based hydrogen storage, and promoter molecular length at C2~C4 are preferred.

(3) Hydrogen and chemical energy storage in HCFC141b + H_2 hydrate

Fig. 5 shown that hydrate-based hydrogen storage capacity of HCFC-141 b + H_2 hydrate in different periods which at 273 K and initial pressure of 12 MPa, 10 MPa, 8 MPa and 6 MPa. For hydrate-based hydrogen storage system at 273 K as well as initial pressure of 12 MPa and 10 MPa, the hydrogen storage capacity could reach one third of the total capacity within 4 h. The gas storage capacity of the system in the first 4 h which at

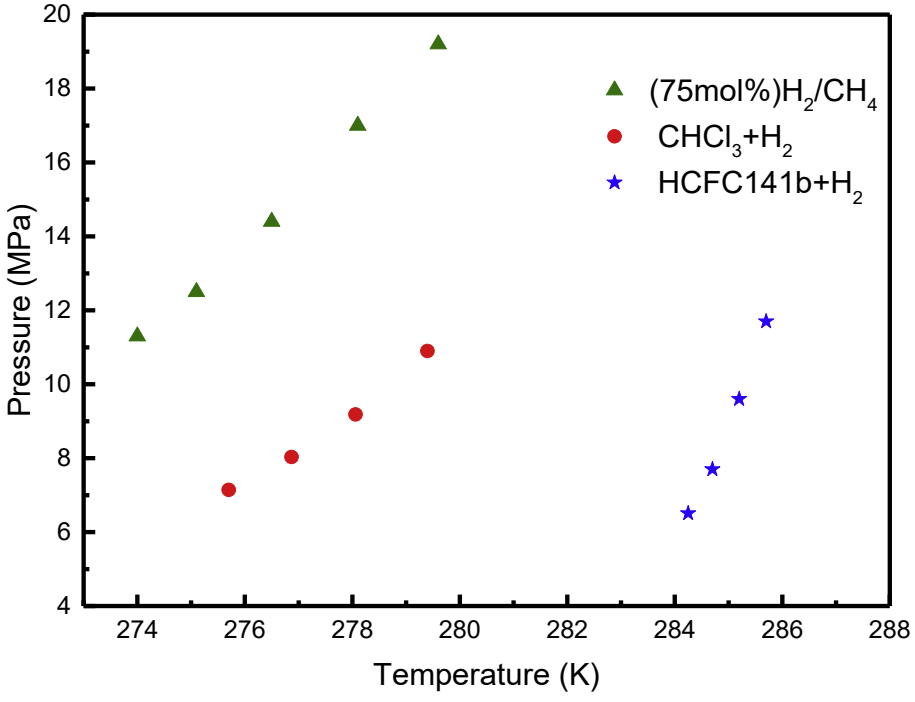

. 4 – 141 + 2+ 3+ 2+ .

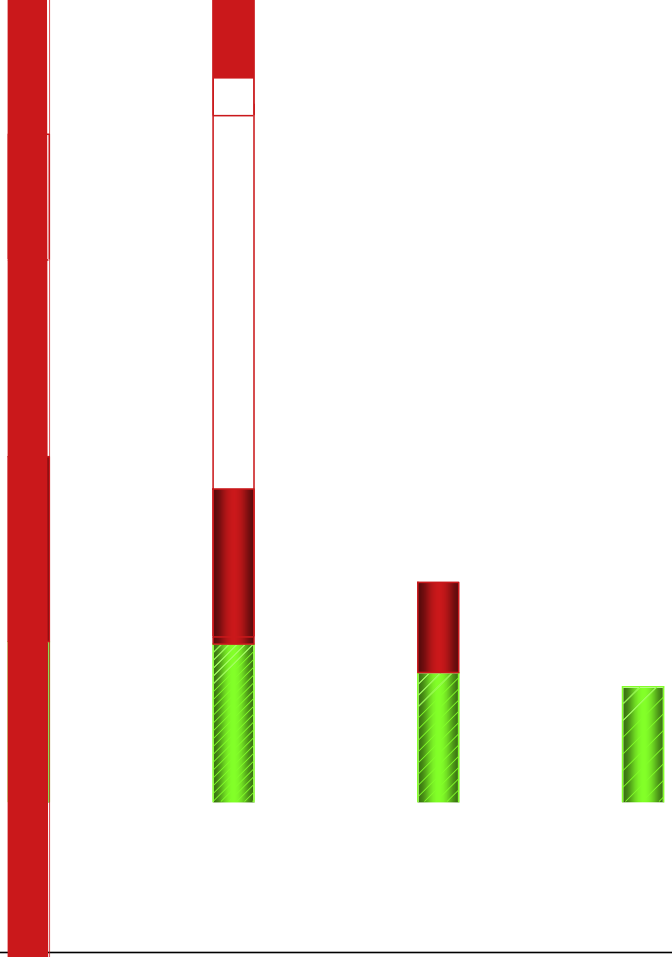

273 K with initial pressure of 12 MPa bout 0%, 24% and 39% higher than that of at 273 k with in pressure of 10 MPa, 8 MPa and 6 MPa respectively. The n on for this phenomenon is that the pressure driving for f 12 MPa system and 10 MPa system is the largest and the h rogen partial pressure is the highest at the beginning of hyd formation. Hydrogen molecule rapidly enters into the s ture II hydrate cage which have been formed by HCFC-1 molecule and water molecule, so the gas storage capacity increased to a certain extent compared with the other two er pressure systems.

In the period of 4–12 h, the hydr n storage capacity of 5.6 mol% HCFC-141 b water mixture rogen storage system at 273 K with initial pressure of 12 M nd 10 MPa increased more than that of with initial press of 8 MPa and 6 MPa. After occupying the emptied 5^{12} ca hydrogen molecules could migrate to $5^{12}6^4$ cages of sII hy te due to the smaller molecules size. During the migration cess the driving force of the systems with initial pressur 8 MPa and 6 MPa is lower than that of 12 MPa and 10 MPa. As the consequences hydrogen storage capacity in 4–12 h of the systems with initial pressure of 12 MPa and 10 MPa remain ahead of that with initial pressure of 8 MPa and 6 MPa. Table 4 shown that after 12 h hydrogen storage systems with initial pressure of 10 MPa has similar hydrogen storage properties comparing to higher pressure system, total hydrogen storage capacity could reach 46 V/V (0.36 wt%).

Conclusions

In this paper enclathration of methane + tert-butyl alcohol, 1,1-dichloro-1-fluoroethane and trichloromethane in hydrogen hydrates were studied. Methane + tert-butyl alcohol (tBA) as a chemical hydrogen storage could significantly thermodynamically enhanced hydrate-based hydrogen storage. 5.6 mol% tBA and 2.8 mol% tBA shifted hydrate phase equilibrium line of (75 mol%) H_2/CH_4 about 4 K and 5 K towards higher temperature, respectively. Raman spectra shows the thermodynamic promotion mechanism was that tBA and water molecules firstly form metastable clathrate cages through hydrogen bonds between hydroxyl groups, then form stable sII hydrates with the help of methane molecules and play a role in thermodynamic promoting the formation of hydrogen hydrates. Phase equilibrium line of hydrogen hydrate shifts 10 K in HCFC-141 b and 5 K in $CHCl_3$ toward higher temperature respectively comparing to (75 mol%) H_2/CH_4 hydrate, which are much milder than hydrogen hydrate phase equilibrium conditions. Besides guest molecular with –F group is better than with -Cl on thermodynamically promoting hydrate-based hydrogen storage. Hydrogen storage capacity of H_2 forming hydrate in 5.6 mol%HCFC-141 b water

mixture at 273 K and 10 MPa could reach 46 V/V (0.36 wt%). Combing with chemical energy of HCFC-141 b, this work achieved high capacity of hydrogen and chemical storage in gas hydrate at mild conditions.

This work was funded by the National Key Research and Development Program (2016YFC0304006, 2017YFC0307302 and 2017YFC0307303), National Natural Science Foundation of China (21736005, 51576069 and 51876069) and. Raman spectra studies were conducted with the assist of Miss Dongmei Wang and Mr. Ke Zhang from ThermoFisher China Co. . The authors sincerely appreciate their contributions to this work.

REFERENCES

[1] Ding J, Cheng Y, Yan C, Song B, Sun H, Teng F. Experimental study of sand control in a natural gas hydrate reservoir in the South China sea. Int J Hydrogen Energy 2019;44:23639–48.
[2] Yan C, Cheng Y, Li M, Han Z, Zhang H, Li Q, et al. Mechanical experiments and constitutive model of natural gas hydrate reservoirs. Int J Hydrogen Energy 2017;42:19810–8.
[3] Guo Y, Pu W, Zhao J, Guo Y, Lian P, Liu Y, et al. Effect of the foam of sodium dodecyl sulfate on the methane hydrate formation induction time. Int J Hydrogen Energy 2017;42:20473–9.
[4] Farhadi A, Mohebbi V. CO2 separation from the mixture of CO2/H-2 using gas hydrates: experimental and modeling. Int J Hydrogen Energy 2017;42:19967–76.
[5] Xia Z, Li X, Chen Z, Yan K, Xu C, Cai J. Hydrate-based hydrogen purification from simulated syngas with synergic additives. Int J Hydrogen Energy 2016;41:2649–59.
[6] Nakayama T, Tomura S, Ozaki M, Ohmura R, Mori YH. Engineering investigation of hydrogen storage in the form of clathrate hydrates: conceptual design of hydrate production plants. Energy Fuels 2010;24:2576–88.
[7] Shibata T, Yamachi H, Ohmura R, Mori YH. Engineering investigation of hydrogen storage in the form of a clathrate hydrate: conceptual designs of underground hydrate-storage silos. Int J Hydrogen Energy 2012;37:7612–23.
[8] Ozaki M, Tomura S, Ohmura R, Mori YH. Comparative study of large-scale hydrogen storage technologies: is hydrate-based storage at advantage over existing technologies (vol 39, pg 1888, 2014). Int J Hydrogen Energy 2014;39:10320–1.
[9] Veluswamy HP, Kumar R, Linga P. Hydrogen storage in clathrate hydrates: current state of the art and future directions. Appl Energy 2014;122:112–32.
[10] Mao WL, Mao HK. Hydrogen storage in molecular compounds. Proc Natl Acad Sci USA 2004;101:708–10.
[11] Mao WL, Mao HK, Goncharov AF, Struzhkin VV, Guo QZ, Hu JZ, et al. Hydrogen clusters in clathrate hydrate. Science 2002;297:2247–9.
[12] Weissman JT, Masutani SM. Hydrogen storage capacity of tetrahydrofuran and tetra-N-butylammonium bromide hydrates under favorable thermodynamic conditions. Energies 2017;10:1225.
[13] Liu J, Hou J, Xu J, Liu H, Chen G, Zhang J. Ab initio study of the molecular hydrogen occupancy in pure H 2 and binary H 2 -THF clathrate hydrates. Int J Hydrogen Energy 2017;42:17136–43.
[14] Di Profio P, Canale V, Germani R, Arca S, Fontana A. Reverse micelles enhance the formation of clathrate hydrates of hydrogen. J Colloid Interface Sci 2018;516:224–31.
[15] Kaur SP, Ramachandran CN. Hydrogen-tetrahydrofuran mixed hydrates: a computational study. Int J Hydrogen Energy 2018;43:19559–66.
[16] Trueba AT, Radovic IR, Zevenbergen JF, Kroon MC, Peters CJ. Kinetics measurements and in situ Raman spectroscopy of formation of hydrogen-tetrabutylammonium bromide semi-hydrates. Int J Hydrogen Energy 2012;37:5790–7.
[17] Trueba AT, Radovic IR, Zevenbergen JF, Peters CJ, Kroon MC. Kinetic measurements and in situ Raman spectroscopy study of the formation of TBAF semi-hydrates with hydrogen and carbon dioxide. Int J Hydrogen Energy 2013;38:7326–34.
[18] Veluswamy HP, Chen JY, Linga P. Surfactant effect on the kinetics of mixed hydrogen/propane hydrate formation for hydrogen storage as clathrates. Chem Eng Sci 2015;126:488–99.
[19] Veluswamy HP, Yew JC, Linga P. New hydrate phase equilibrium data for two binary gas mixtures of hydrogen and propane coupled with a kinetic study. J Chem Eng Data 2015;60:228–37.
[20] Matsumoto Y, Grim RG, Khan NM, Sugahara T, Ohgaki K, Sloan ED, et al. Investigating the thermodynamic stabilities of hydrogen and methane binary gas hydrates. J Phys Chem C 2014;118:3783–8.
[21] Zhang Z, Kusalik PG, Guo G-J. Molecular insight into the growth of hydrogen and methane binary hydrates. J Phys Chem C 2018;122:7771–8.
[22] Qi J, Wang Y, Fan S, Lang X, Li Q, Li G, et al. Hydrate equilibrium measurements for CH4 and CO2/CH4 mixture in the presence of single 2-Methyl-2-propanol and 1,1-Dichloro-1-fluoroethane. J Chem Eng Data 2018;63:3145–9.
[23] Fan S, Li Q, Nie J, Lang X, Wen Y, Wang Y. Semiclathrate hydrate phase equilibrium for CO2/CH4 gas mixtures in the presence of tetrabutylammonium halide (bromide, chloride, or fluoride). J Chem Eng Data 2013;58:3137–41.
[24] Xu S, Fan S, Yao H, Wang Y, Lang X, Lv P, et al. The phase equilibria of multicomponent gas hydrate in methanol/ethylene glycol solution based formation water. J Chem Thermodyn 2017;104:212–7.
[25] Long X, Wang Y, Lang X, Fan S, Chen J. Hydrate equilibrium measurements for CH4, CO2, and CH4 + CO2 in the presence of tetra-n-butyl ammonium bromide. J Chem Eng Data 2016;61:3897–901.
[26] Wei JG, Fang YX, Lu HL, Lu HF, Lu JA, Liang JQ, et al. Distribution and characteristics of natural gas hydrates in the Shenhu sea area, South China sea. Mar Petrol Geol 2018;98:622–8.
[27] Kim E, Lee S, Lee JD, Seo Y. Enclathration of tert-butyl alcohol in sII hydrates and its implications in gas storage and CO2 sequestration. Fuel 2016;164:237–44.
[28] Vos WL, Finger LW, Hemley RJ, Ho-kwang M. Novel H2-H2O clathrates at high pressures. Phys Rev Lett 1993;71:3150–3.